LARGE EDDY SIMULATION OF A HIGHLY TURBULENT METHANE FLAME: APPLICATION TO THE DLR STANDARD FLAME

A. Kempf*, C. Schneider, A. Sadiki, J. Janicka

Dept. of Mechanical Engineering
Institute for Energy- and Powerplanttechnology
TU-Darmstadt, Petersenstr. 30
64289 Darmstadt, Germany

ABSTRACT

A Large Eddy Simulation in three dimensions is applied for the study of a highly turbulent methane flame. As target for this investigation, a flame with simple flow-field that burns without stability problems was a prerequisite, while this flame should not form soot to simplify laser-diagnostics. A good choice for this can be the DLR-Standard-Flame.

In the numerical method for the flow, fluctuations of density in space and time are considered to only depend on chemistry, not on pressure. To represent the sub-grid scale stresses and scalar flux, a Smagorinsky model is used in which the coefficient is determined by the dynamic Germano procedure. Density, temperature and species concentrations are related to the mixture fraction by a flamelet model. Subgrid fluctuation of the mixture fraction is described by a β- function.

The computed results are found in overall agreement with the experimental data. Only close to the nozzle of the fuel-jet gradients are too big to be resolved by the underlying numerics.

INTRODUCTION

Only recent publications show results of full three dimensional LES for chemical reactive flows with varying density (Forkel and Janicka 1999, Hawkes et al. 2000, Steiner and Pitsch 2000). However, these investigations were limited to either hydrogen chemistry or to low turbulent flows. This is necessary because less reactive fuels with strong turbulence would require flame stabilization, which usually leads to more complicated flow fields. Furthermore, less reactive fuels tend to form soot, which is disastrous for laser-diagnostics. To still achieve non-lifted methane flames equally suited for experimental and numerical investigation, Meier (Bergmann et al. 1998) suggested a fuel mixture of methane (33.2 % vol.), hydrogen (22.1 % vol.) and nitrogen (44.7 % vol.). This fuel will burn stable and not form soot when used for a highly turbulent jet flame, which is referred to as DLR-Flame (8 mm of nozzle-diameter, 0.3 m/s velocity in coflow, 15 200 Reynolds number, 0.167 stoichiometric mixture fraction; DLR = German Aerospace Center). This flame is even more interesting since a wealth of experimental data (Bergmann et al. 1998, Meier et al., Flame Database) and simulation results (RANS data by H. Pitsch, O. Kunz and J.-Y. Chen presented in the TNF 5 workshop, poster session) is already available. The work presented here applies LES to this flame and examines its suitability for the simulation of such systems.

*Corresponding author: akempf@gmx.net

GOVERNING EQUATIONS

The numerical scheme applied is based on the Favre-filtered equation of conservation of mass,

$$\frac{\partial \overline{\rho}}{\partial t} + \frac{\partial}{\partial x_j}\left(\overline{\rho}\widetilde{u_j}\right) = 0 \qquad (1)$$

where ρ is density and u_i the velocity component in x_i direction. The over-bar denotes to the filtering in space, while the tilde describes density weighted filtered quantities.

To describe conservation of momentum, the filtered equation (2) is used. In this equation, p denotes the pressure and ν molecular viscosity.

$$\frac{\partial}{\partial t}\left(\overline{\rho}\widetilde{u_i}\right) + \frac{\partial}{\partial x_j}\left(\overline{\rho}\widetilde{u_i}\widetilde{u_j}\right) =$$
$$\frac{\partial}{\partial x_j}\left[\overline{\rho}\widetilde{\nu}\left(\frac{\partial \widetilde{u_j}}{\partial x_i} + \frac{\partial \widetilde{u_i}}{\partial x_j}\right) - \frac{2}{3}\overline{\rho}\widetilde{\nu}\frac{\partial \widetilde{u_k}}{\partial x_k}\delta_{ij}\right] \quad (2)$$
$$+ \frac{\partial}{\partial x_j}\overline{\rho}\tau_{ij}^{\mathrm{SGS}} - \frac{\partial \overline{p}}{\partial x_i} + \overline{\rho}g_i$$

For the description of mixing, the filtered transport equation reads:

$$\frac{\partial}{\partial t}\overline{\rho f} = -\frac{\partial}{\partial x_j}\left(\overline{\rho}\widetilde{f}\widetilde{u}_j + \frac{\overline{\rho}\left(\widetilde{\nu} + \widetilde{\nu}_t\right)}{\sigma_f}\frac{\partial \widetilde{f}}{\partial x_j}\right) \quad (3)$$

In equation (3), f is the mixture fraction, ν_t the turbulent viscosity, and σ_f is the turbulent Schmidt-number.

MODELING AND NUMERICAL PROCEDURE

Flowfield

To solve equations (1-3), an incompressible (i.e. $\partial\rho/\partial p = 0$) 3D LES code, which considers variable density (i.e. $\partial\rho/\partial T \neq 0$; $\partial\rho/\partial f \neq 0$ and thus $\partial\rho/\partial t \neq 0$), is applied.

Following Forkel et al. (1999) and Kempf et al. (2000), equations (1-3) are transformed into cylindrical coordinates and discretized in space by finite volumes using high order central schemes and integrated in time by a 3rd order low-storage Runge-Kutta scheme.

To model the subgrid fluctuation in the velocity field (τ_{ij}^{SGS}), the well known Smagorinsky model (Smagorinsky 1963) is used, with the dynamic Germano procedure (Germano 1991) determining the model coefficient.

Mixing

The transport equation for the mixture fraction (3) only conserves $\overline{\rho f}$, thus this scalar must be split according to a procedure by Forkel (1999) to yield mean density $\overline{\rho}$ and mixture fraction $\widetilde{f}$. Turbulent diffusion is described by a similarity approach with a Schmidt number of $\sigma_f = 0.7$ based on experience (Forkel et al. 1999, Kempf et al. 2000). Subgrid fluctuations of the mixture fraction are modeled by computing the mixture fraction variance over the neighboring cells.

Chemistry

Chemical reaction is considered by a basic flamelet approach. With LES, this is more promising than in RANS context since the naturally thin flamelets are better resolved. Thus, the chemical state is defined by the local mixture fraction, rate of scalar dissipation and the subgrid fluctuation of the mixture fraction. For subgrid distribution, a β-pdf is assumed. For scalar dissipation, a δ-function is used to describe its pdf. For modeling the rate of scalar dissipation, the most basic approach is chosen, modeling χ according to its definition:

$$\chi = 2D\left(\frac{\partial \widetilde{f}}{\partial x_i}\right)^2 \quad (4)$$

With the three known scalars (mixture fraction, rate of scalar dissipation and subgrid fluctuation of mixture fraction), a flamelet table generated by J.-Y. Chen delivers all relevant information on chemical state like density and viscosity, which are used to predict the next time-step of the flowfield. Since the flow-solver applied deals with the stiff system of equations for incompressible flows, it is destabilized by the sudden expansion of fluid elements due to reaction. To stabilize the scheme, an underrelaxation of density (Forkel et al. 1999) in time is performed. Relaxation time is less critical here than in the case investigated by Forkel (1999), so that the relaxation can be improved over $5 \cdot 10^{-4}$ s.

CONFIGURATION AND BOUNDARY CONDITIONS

The flame investigated is a jet diffusion flame as sketched in Figure 1.

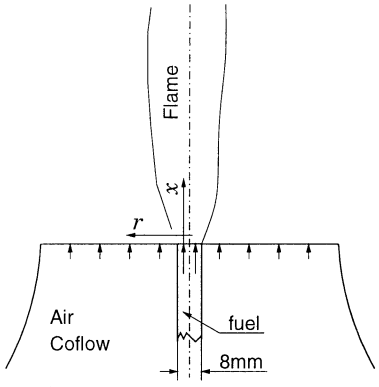

Figure 1: Jet diffusion flame

A central nozzle spends the fuel, while a surrounding air coflow is necessary for experimental reasons: It is needed to provide the LDA-particles (Laser Doppler Anemometry) required for velocity measurements and has the side effect of reducing the influence of external

U_{Jet}	U_{Coflow}	D	X_{CH_4}	X_{H_2}	X_{N_2}
42.2 m/s	0.3 m/s	8 mm	33.2 %	22.1 %	44.7 %

Table 1: Parameters of the DLR-Flame

disturbances onto the flow. The fuel streams of the feeding pipe at a Reynolds-number of $Re = 15,200$, which corresponds to a bulk velocity of 42.2 m/s. The laminar air-coflow streams at a rate of only 0.3 m/s.

The fuel mixture was formulated to make the flame burn stable by adding high-reactive hydrogen and to inhibit soot-formation by the addition of Nitrogen. As described, the fuel consists of 33.2 % vol. methane, of 22.1 % vol. hydrogen and 44.7 % vol. of nitrogen. All Parameters are summarized in table 1.

Experimental investigation of this configuration has been performed by DLR and Sandia Labs for species-fields and EKT (C. Schneider) for velocity-fields.

Computational domain

For the Large Eddy Simulation, a cylindric computational domain of 0.38 m length and 0.48 m in diameter was chosen, just beginning at the exit plane of the nozzle. The nozzle and the coflow were modeled using an inflow condition on the abutting face of the cylinder. This consists of a Dirichlet condition for both velocity and mixture fraction and a von Neumann condition for pressure. To describe the turbulent inflow, a turbulent velocity profile computed by the preceeding LES of a pipe-flow was applied.

The computational domain was discretized with an axis-symmetric grid of $129 \times 32 \times 60$ (axial, tangential, radial) cells. To check if this grid resolution was fine enough, the flow-field at the nozzle was recomputed again with refined cells on a domain of half the previous size ($257 \times 32 \times 60$ cells). Assuming the highest gradients in velocity and mixture appear close to the nozzle, this method is capable to check for "grid-independence" without the need for twice as many cells in each direction (i.e. 16 times more CPU-time, approx. 5 months). This study shows that an almost grid-independent solution had been achieved (see Figures 2 and 3), although it shall be stressed here that there is no "absolute" grid independence to be expected in LES-context since the subgrid model varies with varying filter widths (i.e. cell-size with Schumann-Filtering). With smaller resolved length scales, the modeled part of the turbulence vanishes when Kolmogorov-Scales are resolved. Furthermore, the over-all error from the model will diminish with finer resolution.

RESULTS

In this section we present the main numerical results in comparison to experimental data (if available). The plots presented here are y over x plots only, rendering possible the quantitative comparison of the data. For the scalar and velocity fields, axial and radial profiles of both mean and standard deviation are plot.

Mean values of numerical results are plot with a fat line, its fluctuation with a fine line of corresponding type. For experimental data, a full symbol is used for the mean values, while the same, empty symbol denotes its fluctuation.

Flow-Field

The flow field is presented in figure 2 and figure 3. Figure 2.a shows the axial development of the axial velocity u. Comparing the numerical results to the experimental data, one finds the jet is predicted to "loose" too much momentum. This means the jet would spread faster than in reality. This is confirmed by the plot of the fluctuations, which are significantly over-predicted at $x/D = 10$; i.e. the turbulence and thus momentum "loss" are overestimated.

Although experimental and numerical results generally agree, it is interesting to see how turbulence develops just down-stream the nozzle. The experiments show that the turbulence level in the nozzle is to be expected around 5 %, whereas the simulation predicts a far smaller level. Previous LES studies reveal that cold LES is capable to describe the main characteristics of this type of flow such as mean velocity profiles, the spreading and the dominant frequency at the end of the potential core. However, the turbulence intensities in the self-preservation region showed discrepancies compared to measurements (Hoffman, 1996). Here, the essential features of the turbulence production in the shear layer is well reproduced. The differences observed may be due to these inflow-conditions and to reasonably resolving the high gradients (mixture-fraction field in particular) right at the nozzle.

To check for the influence of the grid-resolution, a computation on a finer grid has been performed. However, to limit computation time[1], the computational domain was shrunk as well to reduce the number of cells.

[1] Reducing each cell to half its size (in each dimension) would result in a computational time of almost one half of a year.

Thus, there only exist results for the finer grid close to the nozzle. This computation will be labeled C2.

To further describe the flow-field, figure 2.b gives some radial profiles of the axial velocities. The first set of data was taken at the plane $x/D = 5$, the second one at $x/D = 20$. The mean profiles at $x/D = 5$ show that the jet tends to spread too much, which is confirmed by the curve at $x/D = 20$. For the fluctuations, the general agreement is sufficing here as well.

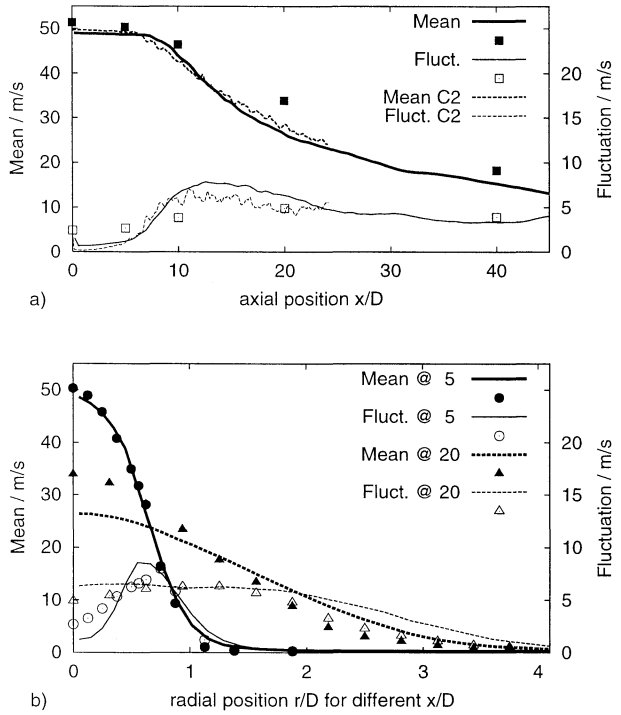

Figure 2: Axial velocities over axis/radius

After axial velocities were presented in Figure 2, both radial and tangential velocities are given in Figure 3. Experimental data is presented as far as available. Figure 3.a shows the axial development of the radial/tangential fluctuations along the axis. Mean velocities are not presented for being 0 on the axis of an axis-symmetric flowfield. Figure 3.b and figure 3.c show radial plots of tangential and radial velocities, respectively.

All in all, the prediction of the flow-field is satisfying, although the results suffer of inaccuracies in the nozzle-area. This well known problem in the literature is connected to the transition from the wall-affected turbulence in the nozzle to the free turbulence, along with a structural change in the turbulence. With RANS modeling, some corrections are generally considered, with regard to the determination of some model parameters (H. Pitsch, O. Kunz and J.-Y. Chen, RANS-Modeling of the DLR-flame, presented in the TNF 5 workshop, poster session). This kind of ad hoc parameter adjustment does not exist in LES using Germano procedure.

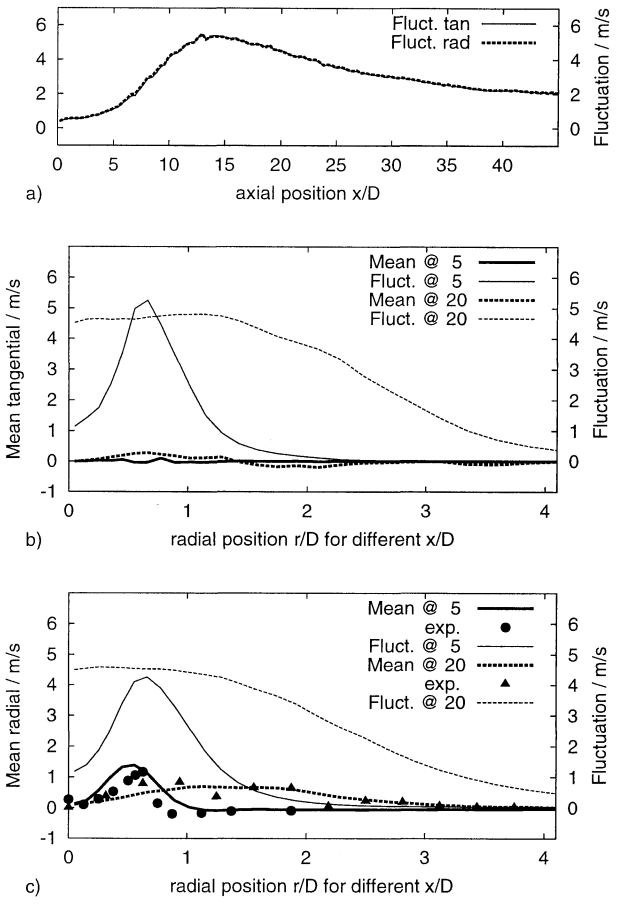

Figure 3: Tangential/Radial velocities over axis/radius

Mixing

Since this work describes chemical processes based on the mixture-fraction approach, the mixing fields shall be presented next. Figure 4 shows the axial and radial profiles of the mixture fraction along the same paths as the velocities presented previously.

Here, evidence is even stronger that the jet breaks up too early, resulting in a strong decay of the mixture fraction along the axis. This is confirmed again by Figure 4.b, which shows too lean mixture at the axis and too rich mixture away from it. Here again, it is interesting to study the axial development of the fluctuation. The predicted curve starts at zero, which corresponds to the jet potential core. At 5 diameters downstream, the jet suddenly breaks up with very high fluctuation. Further downstream, where gradients in the mixture-fraction have

been "smoothed", the prediction of the fluctuation agrees well to the experimental data again.

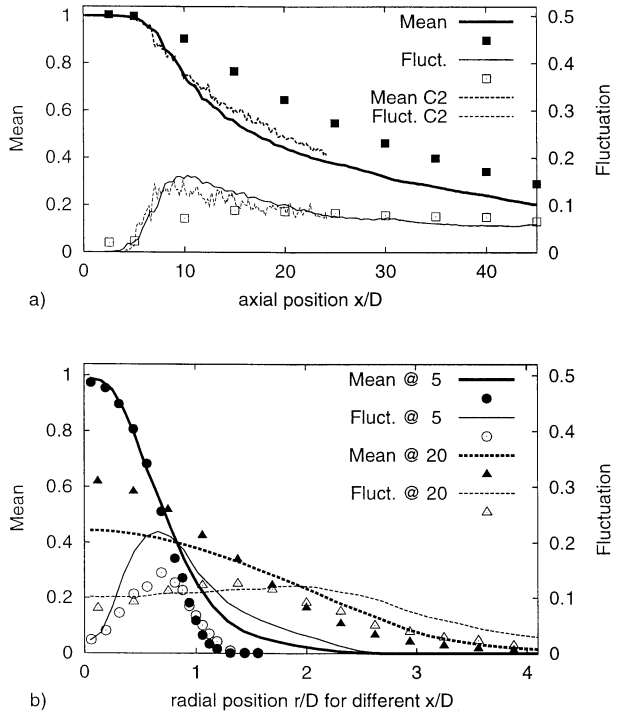

Figure 4: Mixture fraction over axis/radius

Generally, the mixing field shows that the jet breaks up too early. However, this is not really astounding since a study of jet break up requires a very high grid resolution to reasonably resolve the gradients in the mixture fraction field: At the nozzle, the gradient is very high – which can not be resolved by the finer grid neither. This certainly effects the model for the mixture fraction sub-grid variance, which estimates $\widetilde{f''}$ too low when very high gradients occur. Errors in the mixing field (mean and fluctuation) certainly impinge the density fields and thus influence the velocity field as well. This seems to be the main reason why the jet is predicted to spread too strong and to break up early.

Temperature

As one would expect (Figure 5), temperature behaves similar to the mixture fraction, with high temperatures being predicted too early (i.e. too far upstream). Since there is a strong non-linear relation between temperature (or density) and mixture fraction, the error in the prediction of the mixture fraction appears strongly amplified here. This is mainly true for the radial profile of the mean temperature at $x/D = 5$, at a radial position of $r/D \approx 1.5$. There, a temperature of 1000 K is predicted, while the measurements show that this area is not affected by chemical reaction yet.

However, the temperature at the location $(x/D = 5; r/D = 0.9)$ is slightly underpredicted. Further downstream, away from the nozzle-area, the results look much better again, but certainly, they still rely on the predictions at the nozzle.

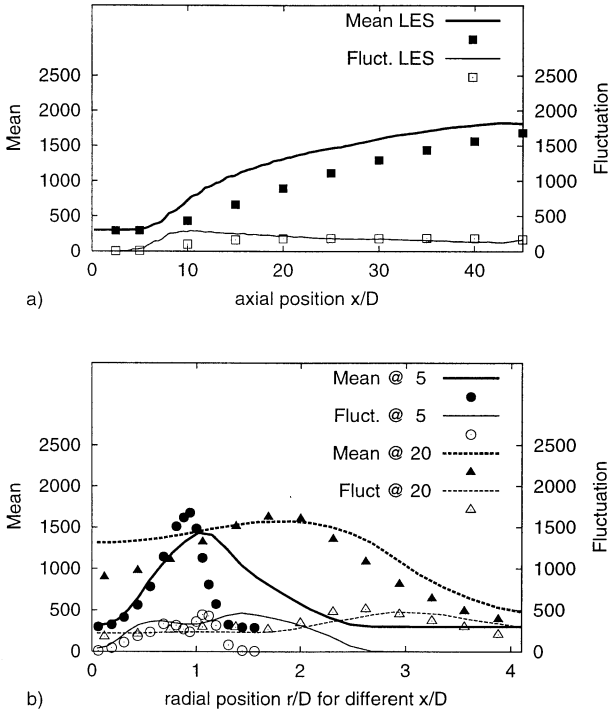

Figure 5: Temperature over axis/radius

Species

Since the main species are defined by the mixture fraction, they all behave similar and thus do not need to be presented. However, flamelet chemistry introduces some interesting information on minor species, so that OH-concentration shall be given here (Figure 6). Considering the axial plot, the trend is certainly predicted. However, the OH concentration on the centerline is overestimated, probably due to the underestimation of the mixture-fraction in the fat regime.

Focusing on radial plots, the results look far better. At $x/D = 5$, OH-concentration is underestimated. This corresponds to the too low temperatures in this area, which have been described in previous section. In the $x/d = 20$ plane, OH-concentration looks very satisfying again.

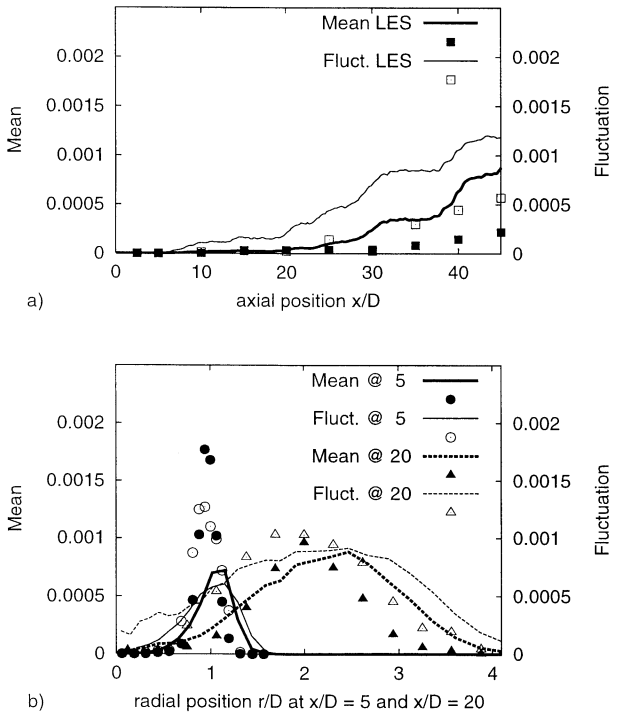

Figure 6: OH-Concentration over axis/radius

CONCLUSIONS

A jet diffusion flame has been simulated by LES to predict its flow-, mixing- and species fields. Considering the results presented here, one finds that LES is well capable of predicting the chemistry in this diffusion flame.

For the main quantities like axial velocity and mixture fraction, good agreement with the measured data is observed in the far field. For the near field, the spreading rate turned out to be sensitive to the inlet condition. This fact needs detailed investigation.

ACKNOWLEDGMENTS

The authors want to express their gratitude for the financial support of the DFG Sonderforschungsbereich SFB 568 "Strömung und Verbrennung in zukünftigen Gasturbinenbrennkammern (Projekt 83)".

REFERENCES

V. Bergmann, W. Meier, D. Wolff, W. Stricker, 1998, Appl. Phys., 66, p. 489

H. Forkel, J. Janicka, 1999, "Large-Eddy Simulation of a turbulent Hydrogen Diffusion Flame", First Symposium on Turbulent Shear Flow Phenomena

M. Germano, U. Piomelli, P. Moin and W.H. Cabot, 1991, "A dynamic subgrid-scale eddy viscosity model", Phys. Fluids A, 3, pp. 1760-1765

E.R. Hawkes, R.S. Cant, 2000, "A Flame Surface Density Approach to Large Eddy Simulation of Premixed Turbulent Combustion", Proc. Combust. Inst. 28

G. Hoffman, 1996: "Engineering Application of LES to free and wall-bounded shear layer", PhD Thesis, TU-München, Germany

A. Kempf, H. Forkel, J.-Y. Chen, A. Sadiki, J. Janicka, 2000, "Large Eddy Simulation of a Counterflow Configuration with and without Combustion", Proc. Combust. Inst. 28

W. Meier, R. Barlow, Y.-L. Chen, J.-Y. Chen, 2000, "Raman/Rayleigh/LIF Measurements in a Turbulent CH4/H2/N2 Jet Flame: Experimental Techniques and Turbulence Chemistry Interaction", Combustion and Flame 123, pp. 326-343

N. Peters, 1986, "Laminar Flamelet Concepts in Turbulent Combustion", Proc. Combust. Inst. 21: pp. 1231-1250

C. Schneider, A. Dreizler, J. Janicka, 2000, "LDV-Measurements in Hydrocarbon Air Jet Flames", Private Communication. For data, please contact one of the following:
`cschneid@hrz2.hrz.tu-darmstadt.de`
`dreizler@hrz2.hrz.tu-darmstadt.de`.

H. Steiner, H. Pitsch, 2000, "Large-Eddy Simulation of a Turbulent Piloted Methane/Air Diffusion Flame (Sandia Flame D)", accepted for publication in Physics of Fluids.

J.S. Smagorinsky, 1963, "General circulation experiments with the primitive equations, 1. The basic experiment", Monthly Weather Rev.l, 91, pp. 99-164.

Flame Database:
`http://www.ca.sandia.gov/tdf/DataArch/DLRflames/DLRflames.html`